Determination of potential energy surfaces for Ar–HCl and Kr–HCl from rotational linebroadening data

Joost G. Kircz, Gerald J. Q. van der Peyl, and Jan van der Elsken

Laboratorium voor Fysische Chemie, University of Amsterdam, Nieuwe prinsengracht 126, Amsterdam, Holland

Daan Frenkel

Department of Chemistry, University of California, Los Angeles, California 90024
(Received 24 January 1978)

Using recent rotational linebroadening data at different temperatures of HCl–Ar and HCl–Kr mixtures, an attempt is made to determine anisotropic intermolecular potential surfaces for both systems. The parameters characterizing the anisotropic part of the potential were determined from numerical fitting of computed linebroadening cross sections using the model of Smith, Giraud, and Cooper. The potential for HCl–Ar obtained that way is found to be rather different from potential surfaces that have been put forward in the literature. A comparison between the different potentials is made. In the HCl–Kr case no other "experimental" potential surfaces are available for comparison.

I. INTRODUCTION

The broadening of pure rotational transitions of molecules by perturbing gases is determined by the anisotropy of intermolecular potentials. For this reason the study of rotational line broadening provides us with information about the angle dependent part of the intermolecular interactions. Over the past two decades a considerable amount of theoretical work has been done to obtain quantitative relations between the parameters characterizing a given intermolecular potential and the corresponding cross sections for line broadening.

In this paper we shall apply the results of these efforts and consider the information about the potential which can be obtained in an actual case. In the following we will be concerned with the broadening of rotational transitions of a linear molecule due to interaction with spherical particles. The angle dependent intermolecular interaction between a linear and spherical molecule may, quite generally be expressed by the following expansion:

$$V(r,\theta)=\sum_{l=0}^{\infty}V_l(r)P_l(\cos\theta)\ , \tag{1}$$

where r is the length of the vector joining the centers of mass of the two molecules, θ the angle between this vector and the axis of the linear molecule, and P_l the lth Legendre polynomial. In many instances the anisotropic intermolecular potential $V(r,\theta)$ is assumed to be expandable in a multipole series.[1] Relations between the cross sections for line broadening and the multipole moments are computed through use of a suitable model.[2] One objection that may be raised against the use of a multipole series to describe the intermolecular potential is that this series is known to converge poorly,[3] especially for small r. This means that many multipole moments are needed to characterize the attractive part of the intermolecular potential at short r. In the region where the molecular charge distributions start to overlap, the multipole series fails completely. In other words, the multipole series is probably not the most economic way to parametrize the intermolecular potential in the range that is relevant for line broadening.

Another empirical parametrization of the intermolecular potential has been used by Neilsen and Gordon[4] in their extensive semiclassical trajectory calculations on the HCl–Ar system. These authors assume that all l, $V_l(r)$ may be written as $V_l(r)=a_l^S V_l^S(r)+a_l^L V_l^L(r)$ where S and L stand for short and long range, respectively. The short range part is assumed to have an exponential r dependence, whereas the long range part is assumed to fall off as $1/r^n$, with n chosen such that it is in agreement with the dependence of the leading multipole terms at large r (e.g., $n=7$ for $l=1$, $n=6$ for $l=2$). The constants a_l^S and a_l^L are adjustable parameters. In their paper, Neilsen and Gordon determined a set of parameters that give an optimal fit with the specific experimental data. However, the Neilsen and Gordon calculations are very time consuming and therefore ill suited to be used in a numerical minimization routine. Over the past few years, new experimental information on the rotational line broadening of HCl by Ar and Kr has been obtained.[5,6] In order to interpret this information in terms of potential parameters we wish to use a numerical routine to minimize the weighted mean square difference between experimental and computed linewidths. In doing so, one is obviously forced to compromise between costs and accuracy. The Neilsen and Gordon procedure, although it seems to be the best model available, would be prohibitively expensive, whereas fast simple models for line broadening, like for instance the Anderson model using the straight path approximation,[2] are not very reliable for the HCl–noble gas systems. Recently, Smith, Giraud, and Cooper (SGC)[7] have published an approximate method to compute rotational linewidths, which seems to work well for the HCl–Ar system. Using this method which is much less time consuming than the Neilsen and Gordon calculation, they obtain results for the line broadening of HCl by Ar that agree well with the Neilsen and Gordon results, except for the lowest rotational transitions. In the following we will describe how, using the SGC method, we obtained parameters for the HCl–Ar anisotropic potential surface that are compatible with the new experimental data in Refs. 5 and 6. In the next section some features of the SGC method that have a direct bear-

 0021-9606/78/6910-4606$01.00

ing on the computational procedure are discussed; however, for details the reader is referred to Ref. 7. Section III deals with the actual numerical procedure. The results of the calculations are discussed in Sec. IV.

II. RELATION BETWEEN LINEWIDTH AND INTERMOLECULAR POTENTIAL

The halfwidth at halfheight (HWHH) of a pressure broadened rotational transition is related to the cross section through the following relation:

$$(\Delta\nu_{1/2})_j = (2\pi c)^{-1}\bar{v}_{\rm rel}\sigma_j(T)\rho \ , \tag{2}$$

where $(\Delta\nu_{1/2})_j$ is the HWHH of the rotational transition $j \to j'$ expressed in $\rm cm^{-1}$, $\bar{v}_{\rm rel}$ is the average relative velocity of rotor and perturber molecules, $\sigma_j(T)$ is the temperature dependent cross section for line broadening of the $j \to j'$ transition and ρ is the number density of the perturber gas. The range of validity of the assumptions underlying this expression is discussed in some detail in Ref. 4. The temperature dependent cross section $\sigma_j(T)$ is related to the cross section for line broadening at fixed relative kinetic energy $\sigma(E)_j$ by:

$$\sigma_j(T) = (kT)^{-2}\int_0^\infty \sigma_j(E)\, E \exp(-E/kT)\, dE \ . \tag{3}$$

When the translational degrees of freedom are treated classically $\sigma_j(E)$ is actually an integrand of scattering matrices over all impact parameters b,

$$\sigma_j(E) = \int_0^\infty 2\pi b \sigma_j(E, b)\, db \ . \tag{4}$$

$\sigma(E, b)$ may be expressed in terms of the classical path S matrices corresponding to relative kinetic energy E and impact parameter b.[2,4,7]

In Ref. 7 an approximate expression for the S matrix is developed. One of the main approximations is the fact that it is assumed that the increments $\delta_k = (j_k - j_{k-1})$ are small compared to j_k themselves, where j is the rotational quantum number. This approximation makes the method unsuitable for calculation of the first and second rotational transition. The anisotropic intermolecular potential is contained in the integrals,

$$\int_0^\infty V_l[r(t)]\cos(\omega\delta t)\, dt = V_l(\omega\delta) \tag{5}$$

where δ numbers a series of analytical expressions developed in Ref. 7. $V_l(\omega\delta)$ is the cosine transform of the strength of the lth term in the Legendre polynomial expansion of the intermolecular potential computed along a classical trajectory with given E and b; $t=0$ corresponds to the moment of closest approach. As the computation of the classical trajectories is actually the most time consuming step in the whole computation, it is obviously profitable to parametrize the intermolecular potential in such a way that the trajectory calculations and the cosine transform need not to be redone for every new set of potential parameters. To this end we choose the intermolecular potential to be of the following form:

$$V(r, \theta) = V_0(r) + \sum_{l=1}^{\infty}[a_l^S V_l^S(r) + a_l^L V_l^L(r)]P_l(\cos\theta) \ . \tag{6}$$

The isotropic potential $V_0(r)$ is kept fixed. As the classical paths are calculated with $V_0(r)$, this implies that the classical trajectories have to be computed only once. Although keeping $V_0(r)$ fixed will certainly limit the flexibility of the fitting procedure, this need not be a serious drawback as $V_0(r)$ has been determined (at least in the HCl–Ar case) from other experiments.[4,8,9] The linear parametrization of the anisotropic part of the potential has the advantage that a cosine transform has to be performed only once to yield

$$V_l^S(\omega\delta) = \int_0^\infty V_l^S[r(t)]\cos(\omega\delta t)\, dt \ ,$$
$$V_l^L(\omega\delta) = \int_0^\infty V_l^L[r(t)]\cos(\omega\delta t)\, dt \ , \tag{7}$$

for any choice of a_l^S and a_l^L.

$V_l(\omega\delta)$ is given by $V_l(\omega\delta) = a_l^S V_l^S(\omega\delta) + a_l^L V_l^L(\omega\delta)$. (8)

With this parametrization of the intermolecular potential, $\sigma_j(E, b)$ may be computed efficiently for any choice of the set $\{a_l^S, a_l^L\}$. The cross section $\sigma_j(T)$ is obtained by numerical integration of Eq. (3). As $\sigma(E, b)$ is essentially zero for $b > 4\sigma$ (as appears in the calculations in Ref. 4 where σ is the Lennard-Jones diameter), the integration over b can be performed using a Gauss–Legendre quadrature[10] to compute

$$\sigma_j(E) = \pi\int_0^{b^2_{\rm max}} \sigma_j(E, b)\, db^2 \ .$$

To this end $\sigma(E, b)$ is computed for 40 different trajectories: 4 different E's (128 K, 354 K, 691 K and 1300 K) and 10 different b's for every E (.77 Å, 1.76 Å, 2.71 Å, 3.61 Å, 4.42 Å, 5.15 Å, 5.74 Å, 6.21 Å, 6.55 Å, 6.74 Å).

By suitable change of variables the integral, Eq. (3) can also be cast in a form that is suitable for numerical interpretation using the Gauss–Legendre quadrature,

$$\sigma(T) = \int_0^1 \sigma(E)\, dy \text{ with } y = (-1 - E/kT)\exp(-E/kT) + 1 \ . \tag{9}$$

It should however be noted that the Gauss–Legendre quadrature requires the value of the integral computed at a number of fixed values of the parameter y (for $n=4$, as in our case, $y = 0.6943$, 0.33001, 0.66999, 0.93057, corresponding to the four energies mentioned above for $T = 300$ K). This relation is, however, dependent on the temperature T. This would imply that to compute $\sigma(T)$ at different T's one would have to do a new set of trajectory calculations with different E's. This complication may be eliminated in the following way. Suppose $\sigma(E)$ has been computed at the set of values of the energy that corresponds to a given choice of the temperature T. Then the cross sections at a different temperature T may be written as

$$\sigma(T') = (T/T')^2\int_0^1 \sigma(E)\exp(E/kT - E/kT')\, dy \ , \tag{10}$$

i.e., $\sigma(T')$ may be obtained by quadrature of the function $(T^2/T'^2)\sigma(E)\exp(E/kT - E/kT')$, evaluated at the *same values* for the energy as were required for the computation of $\sigma(T)$. This method will work provided that T' is of the same order of magnitude as T. Test

calculations show that the method is correct for $T' \leq T$, within less than 0.5%.

III. DETERMINATION OF POTENTIAL PARAMETERS

In the previous section we discussed the parametrization of the intermolecular potential,

$$V_0(r,\theta) = V_0(r) + \sum_{l=1}^{\infty} (a_l^S V_l^S(r) + a_l^L V_l^L(r)) P_l(\cos\theta) \ . \qquad (6)$$

In this section we describe how anisotropic potential parameters were obtained from rotational line broadening data on the HCl–Ar and HCl–Kr system. For the HCl–Ar system, Farrar and Lee[8] interpreted molecular beam scattering data in terms of an isotropic potential. Holmgren, Waldman, and Klemperer[9] obtained an isotropic potential for HCl–Ar through a least squares fit of molecular beam electric resonance data on the HCl–Ar dimer. This isotropic potential turns out to be very similar to the one obtained by Farrar and Lee. In our calculations of the line broadening of HCl by Ar we assumed that the true isotropic potential was adequately described by the expression given by Holmgren *et al.* with $\epsilon_0 = 132\ \mathrm{cm}^{-1}$,

$$V_0(r) = \epsilon_0\{6/(\alpha_0 - 6)\exp[\alpha_0(1 - r/r_{\min,0})] - \alpha_0/(\alpha_0 - 6)(r_{\min,0}/r)^6\} \ , \qquad (11)$$

$r_{\min,0} = 3.883$ Å and $\alpha_0 = 14.5$, where ϵ_0 is the minimum well depth and $r_{\min,0}$ the distance at this point for the isotropic part of the potential. [We used the Holmgren, Waldman, and Klemperer (HWK) $V_0(r)$ rather than the Farrar and Lee expression, for reasons of computational convenience.] The isotropic part of the potential was kept the same in all calculations; only the anisotropic part of the potential was varied.

For the Kr–HCl system, no such accurate isotropic potentials are available at present. For this reason we assumed that the isotropic Kr–HCl potential could be adequately described by a Lennard-Jones (12–6) potential

$$V_0(r) = 4\epsilon[(\sigma/r)^{12} - (\sigma/r)^6] \ , \qquad (12)$$

using the Lorentz–Berthulot combination rules:

$$\epsilon_{\mathrm{HCl-Kr}} = (\epsilon_{\mathrm{HCl}} \cdot \epsilon_{\mathrm{Kr}})^{\frac{1}{2}} = 166.1\ \mathrm{cm}^{-1} \ ,$$

$$\sigma_{\mathrm{HCl-Kr}} = (\sigma_{\mathrm{HCl}} + \sigma_{\mathrm{Kr}})/2 = 3.46\ \text{Å} \ .$$

The values for ϵ and σ were taken from Ref. 11. This procedure is known to be accurate to about 5% for the Ar–HCl case. However, in order to test to what extent approximations in the isotropic potential affected the anisotropic parts of the potential, we also did a fit of the Ar–HCl data, using the approximate Ar–HCl L.J. (12–6) isotropic potential obtained from the combination rules $\epsilon_{\mathrm{HCl-Ar}} = 140.4\ \mathrm{cm}^{-1}$ and $\sigma_{\mathrm{HCl-Ar}} = 3.39$ Å.

For both systems, the long and short range parts of the anisotropic potential were assumed to be proportional to the attractive and repulsive parts of the isotropic potential, i.e.,

$$V_l^S(r) \sim 4\epsilon(\sigma/r)^{12} = V_0^R(r) \ ,$$
$$V_l^L(r) \sim 4\epsilon(\sigma/r)^{6+m} = V_0^A(r)(\sigma/r)^m \ , \qquad (13a)$$

in the Lennard-Jones case, and

$$V_l^S(r) \sim 6\epsilon_0/(\alpha_0 - 6)\exp[\alpha_0(1 - r/r_{\min,0})] = V_0^R(r) \ ,$$
$$V_l^L(r) \sim -\epsilon_0\alpha_0/[\alpha_0 - (6+m)](r_{\min,0}/r)^{6+m} = V_0^A(r)(r_{\min,0}/r)^m \ , \qquad (13b)$$

whenever the HWK isotropic potential was used. For the sake of consistency with the long range behavior of the multipole expansion of the anisotropic intermolecular potential, m in Eq. (13a) and (13b) was chosen to be 1 for $l=1$ and 0 for $l=2$.

It should be noted that the separation of the isotropic potential into attractive and repulsive parts is not unique, and other separations have been found to be advantageous in a different case.[12] The present separation is, however, the one that requires the least amount of computing time in fitting the linewidths. Using the above separation of the isotropic intermolecular potential, the total intermolecular potential may now be written as

$$V(r,\theta) = V_0^R(r)(1 + P_1 R\, P_1(\cos\theta) + P_2 R\, P_2(\cos\theta) + \cdots) + V_0^A(r)(1 + P_1 A\,(d/r)\, P_1(\cos\theta) + P_2 A\, P_2(\cos\theta)\cdots) \ , \qquad (14)$$

with $d = \sigma$ in the Lennard-Jones case and $d = r_{\min,0}$ in the other case. The multiplicative parameters $P_l R$ and $P_l A$ may be expected to be of order 1. Multiplicative parametrization of anisotropic intermolecular potentials has recently been criticized by Le Roy *et al.*,[13] because such a parametrization was found to give rise to rather pronounced statistical correlations between the different potential parameters. Nevertheless, we did use multiplicative parametrization because other methods would have required more computing time. It should be added that for the small number of independent parameters we used in the actual fitting procedure, no strong correlation between the parameters was found.

Neilsen and Gordon observed that in their calculations of the collisional line broadening of HCl by Ar, the contribution of the $l=3$ term in the anisotropic interaction to the line broadening was negligible. For this reason we started our determination of the potential parameters assuming all terms in $V(r,\theta)$ with $l \geq 3$ to be identical to zero. We made this assumption not because there is any physical reason to assume these higher terms to be zero, but rather to see whether a satisfactory fit of experimental data could be obtained with the $l=1$ and $l=2$ terms only. The actual computation consisted of minimizing the weighted sum of squared differences between the computed and experimental line broadening crosssections,

$$F = 1/N \sum_{\alpha=1}^{N} W_\alpha[\sigma_\alpha(\mathrm{exp}) - \sigma_\alpha(\mathrm{calc})]^2 \ , \qquad (15)$$

where α numbers the measured transitions at the different temperatures used in the experiments of Ref. 5 and 6. The weight factors are equal to 1/(estimated experimental error in σ_α)^2.

Errors introduced into the computation through the approximate nature of the SGC model are hard to assess. As mentioned already, the calculations by Smith,

TABLE I. Potential parameters.

	Potentials determined by fitting procedure in this article			Proposed potentials to be found in the literature: e, Ref. 4; HWK1 and HWK2, Ref. 9.				
	Ar–HCl		Kr–HCl	Ar–HCl				Kr–HCl
	A1[a]	A2[b]	K	e	HWK1	HWK2	multipole	multipole
P_1A	0.61 ± 0.10	0.63 ± 0.12	0.54 ± 0.17	0.32	1	1	0.26	0.29
P_1R	0.55 ± 0.08	0.55 ± 0.09	0.41 ± 0.14	0.51	1	1		
P_2A	0.39 ± 0.04	0.37 ± 0.02	0.29 ± 0.06	0.24	1	1	0.063	0.064
P_2R	0.22 ± 0.08	0.37 ± 0.09	0.15 ± 0.14	0.78	1	1		
ϵ_0(cm^{-1})	132.0	140.39	165.95	140.39	131.2	132.0		
$r_{\min,0}$(Å)	3.883	3.805	3.90	3.805	3.804	3.883		
α_0	14.5	···	···	13.5	17.9	14.5		
ϵ_1	91.1	84.6	99.89	28.3	52.6	19.0		
$r_{\min,1}$	3.75	3.65	3.65	4.0	4.123	3.866		
α_1	14.5	···	···	13.5	9.75	12.4		
ϵ_2	79.3	51.4	93.0	14.82	23.5	43.4		
$r_{\min,2}$	3.60	3.80	3.50	4.45	4.123	4.189		
α_2	14.5	···	···	13.5	8.5	14.1		

[a]A modified Buckingham type potential.
[b]A Lennard-Jones type potential. ϵ_l is the well depth; $l=0$, isotropic part; $l=1$, P_1 part; $l=2$, P_2 part all for $\theta=0°$ $r_{\min}$, l is the distance for ϵ_l; and α_l a constant in the case of a modified Buckingham type potential.

Giraud, and Cooper[7] indicate that the model does not give accurate results for the lowest two rotational transitions ($J=0\rightarrow 1$) and ($J=1\rightarrow 2$), so we excluded the cross sections for these transitions from the fitting procedure. In minimizing F the parameters P_1A, P_1R, P_2A, and P_2R were varied independently. The minimization routine that we used was taken from the Cern Computer 7500 Interim Program Library. From this library we used the so called "Minuit" minimization procedure,[14] in particular the routines "simplex" and "migrad." To test for possible local minima in F, several runs with different initial values of the parameters were performed. The set of parameters that gives the best fit with the experimental data is independent of initial conditions and is tabulated in Table I. Parabolic error estimates, taking possible statistical correlations between the potential parameters into account[15] are also shown in Table I. Computed line broadening cross sections for the best fit potentials are displayed in Figs. 1 and 2, together with the experimental cross sections, the values are tabulated in Tables II and III. In these figures, the estimated experimental errorbars are indicated. Clearly, the data are fitted within experimental accuracy; inclusion of higher l terms in the intermolecular potential is therefore not warranted. Also shown in Fig. 1 are the computed Ar–HCl line broadening cross sections obtained by optimizing the fit to the experimental data, using the Lennard-Jones form [Eqs. (13a) and (14)] for the Ar–HCl isotropic potential. In the following we refer to this latter best fit potential as A2, the best fit potential with the HWK isotropic part will be referred to as A1 and the potential that fitted the Kr–HCl data best will be called K. The fitruns were done on the CDC 6400 computer of the Zeeman laboratory in Amsterdam and took between 5000 and 9000 sec. The other calculations were done on the CDC cyber 73-28 and 173-8 of the academical computer centre (SARA).

IV. DISCUSSION OF THE RESULTS

Figures 3 and 4 give an impression of the overall accuracy with which the Ar–HCl and Kr–HCl intermolecular potential surfaces have been obtained through the fitting procedure described in the previous section. Displayed is the r dependence of $V(r,\theta)$ at $\theta=0$. The drawn lines are the best fit potentials, the width of the shaded area is a measure of the overall uncertainty in this potential. The width of the shaded area was obtained by combining all the errors given in Table I in such a way that they reinforce one another. Although this error estimate is probably somewhat pessimistic (assuming all errors statistically independent, the upper and lower bounds correspond to 4 standard deviation limits), one is forced to conclude that the overall accuracy is disappointing. It should be noted that this lack of accuracy in determining the potential surface is not likely to be very model dependent. Rather it is a reflection of the fact that, at present, line broadening data are just not accurate enough to really pin down the intermolecular potential surface. Yet, in spite of this lack of accuracy, it is nevertheless possible to reach a number of significant conclusions, by comparing the best fit potentials A1, A2 and K with a number of potentials that have been proposed in literature. First, however, we will discuss the effect of the choice of the isotropic potential param-

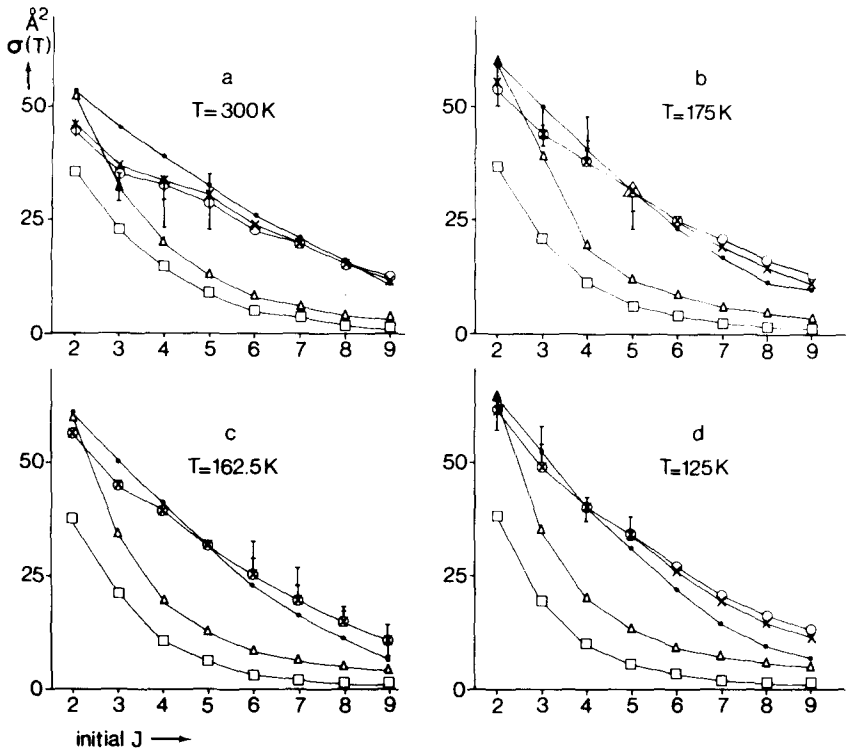

FIG. 1. Cross sections at different temperatures for HCl–Ar. The experimental points are indicated with errorbars. The calculated ones as follows ×A1, ○A2, ● *e*, □ HWK1, △ HWK2 (see text).

eters that yield the best fit. This effect is interesting for two reasons. First of all, as has been mentioned before, we had to use an approximate isotropic potential for the Kr–HCl system. It is clearly important to know whether the effective anisotropic potential surface that corresponds to the best fit for a given approximate isotropic potential may or may not be expected to differ greatly from the "true" anisotropic potential surface. Secondly, a number of the anisotropic potentials as for the Ar–HCl system that have been described in the literature[4,8,9] were obtained assuming a somewhat different Ar–HCl isotropic potential from the one used in the present work. Consequently, comparing these anisotropic potentials with the present ones is, in principle, not fully consistent. It is therefore essential to know whether a meaningful comparison between anisotropic potentials corresponding to different isotropic potentials can still be made. In the previous section we described how best fit anisotropic potential surfaces for the HCl–Ar system were obtained, starting from two different isotropic potentials. In one case (potential A1) the supposedly accurate isotropic potential given by Holmgren *et al.*[9] was used, in the other case (potential A2) we used a Lennard-Jones isotropic potential, obtained through use of the combination rules [Eq. (12)] as in the Kr–HCl case. Figure 3 shows the r dependence for $\theta = 0$ of potential A2. In the same figure, the r dependence of potential A1 is shown. It is observed

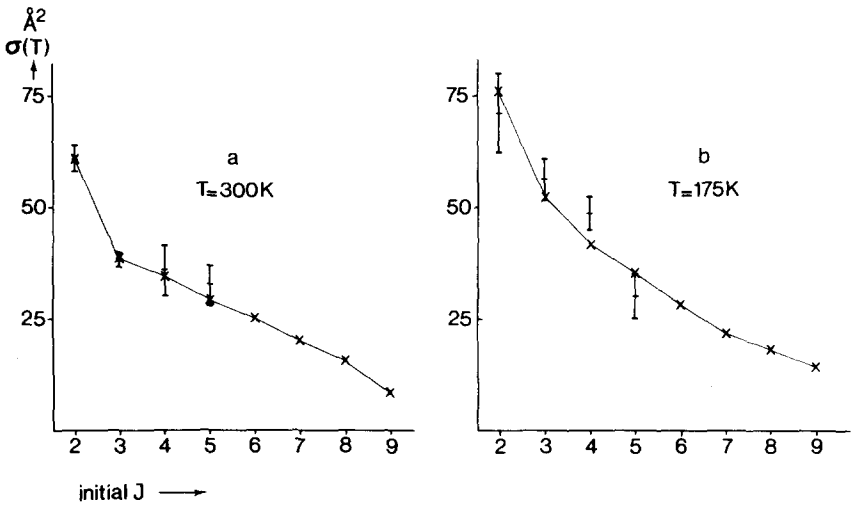

FIG. 2. Cross sections at different temperatures for HCl–Kr. The experimental points are indicated with errorbars. The calculated potential K (see text) with ×.

TABLE II. Cross sections for Ar–HCl as calculated in this article.

Initial J	Experimental	A1	A2	e	HWK1	HWK2
$T=300\,°K$						
2	45.52 ± 2.44[a]	45.96	44.96	53.97	35.87	53.16
3	32.02 ± 3.71	37.15	35.16	45.75	23.31	32.94
4	29.30 ± 5.85	34.68	32.29	38.67	14.59	19.99
5	29.14 ± 6.20	30.43	28.62	32.34	8.91	12.36
6		25.48	24.39	26.45	5.40	7.00
7		20.69	20.21	21.02	3.28	5.49
8		16.49	16.52	16.28	2.04	4.02
9		12.99	13.36	12.39	1.33	3.13
$T=175\,°K$						
2	54.58 ± 4.38[a]	55.16	54.60	60.45	37.28	60.00
3	46.00 ± 4.60	44.05	43.43	50.04	21.03	34.20
4	43.42 ± 4.60	38.85	38.11	41.06	11.26	19.73
5	27.60 ± 4.60	32.23	32.02	32.21	6.08	12.43
6		25.54	25.91	24.02	3.47	8.65
7		19.72	20.51	17.24	2.14	6.50
8		15.08	16.11	12.06	1.45	5.14
9		11.56	12.69	8.34	1.06	4.20
$T=162.5\,°K$						
2		56.63	56.23	61.38	37.48	60.93
3		45.08	44.74	50.68	20.75	34.42
4		39.47	39.04	41.40	10.89	19.83
5		32.53	32.60	32.15	5.81	12.59
6	29.8 ± 4.5[b]	25.63	26.25	23.65	3.31	8.86
7	23.1 ± 4.3	19.70	20.71	16.72	2.07	6.72
8	17.1 ± 1.8	15.02	16.23	11.53	1.42	5.34
9	11.6 ± 4.3	11.52	12.78	7.88	1.05	4.37
$T=125\,°C$						
2	60.69 ± 3.29[a]	61.77	62.17	64.53	38.13	64.03
3	53.61 ± 3.97	48.60	49.44	52.88	19.84	35.20
4	39.69 ± 2.48	41.58	42.36	41.49	9.82	20.36
5	35.42 ± 2.51	33.60	34.78	31.80	5.11	13.34
6		26.04	27.63	22.29	2.97	9.71
7		19.79	21.62	14.96	1.95	7.35
8		15.04	16.92	9.84	1.41	6.06
9		11.58	13.39	6.48	1.09	5.00

[a]Reference 5. [b]Reference 6.

that the two best fit potentials are somewhat different, though within each others maximum error limits. To show the effect of the choice of the isotropic potential on the purely anisotropic part of the potential, the $l=1$ and $l=2$ parts of potentials A1 and A2 have been displayed separately in Fig. 5. In both figures, the shaded area is enclosed by the maximum error estimates in the $l=1$ and $l=2$ parts of the potentials. It is observed that both the $l=1$ and the $l=2$ parts fall within the shaded area, although the difference between the two $l=2$ parts is considerable. Figure 4 suggests the order of magnitude of the error that one may expect to be introducing in the Kr–HCl anisotropic potential, by using the combination rules to generate the Kr–HCl isotropic potential. Figure 6 shows the $l=1$ and $l=2$ parts for the Kr–HCl case. From Figs. 5 and 6 we can also obtain an estimate of the error in the position of the minimum of the $l=1$ and $l=2$ anisotropic potentials. The upper (lower) limit of the shaded area is formed by the potential curve representing the estimated bounds to the repulsive and attractive part of the $l=1, 2$ potentials. Consequently, the positions of the minima of the upper and lower curves provide us with estimates of the upper and lower bounds to $r_{\min}$ for the $l=1, 2$ potentials. Similarly, the upper and lower bounds for $r_{\min}$ of $V(r,\theta)$ for $\theta=0$ can be read directly from Fig. 3. These estimated upper and lower bounds for the position of the minima, together with the corresponding upper and lower bounds of the well depths, are given in Table IV. It is remarkable that deeper minima in all cases coincide with smaller distances at which this minimum occurs, even although all parameters $\{P_l R, P_l A\}$ are statistically independent.

In the introduction it was mentioned that a multipole expansion could not be expected to give an adequate de-

TABLE III. Cross sections for Kr–HCl, as calculated in this article.

Initial J	Experimental[a]	K
$T=300\,°K$		
2	61.56 ± 3.16	61.07
3	38.53 ± 1.92	39.96
4	36.85 ± 6.73	34.97
5	33.09 ± 7.10	30.21
6		25.13
7		20.42
8		16.40
9		13.11
$T=175\,°K$		
2	71.58 ± 8.93	76.21
3	56.24 ± 4.80	51.56
4	49.05 ± 4.80	2.77
5	29.99 ± 4.80	35.20
6		28.24
7		22.40
8		17.79
9		14.27

[a]Reference 5.

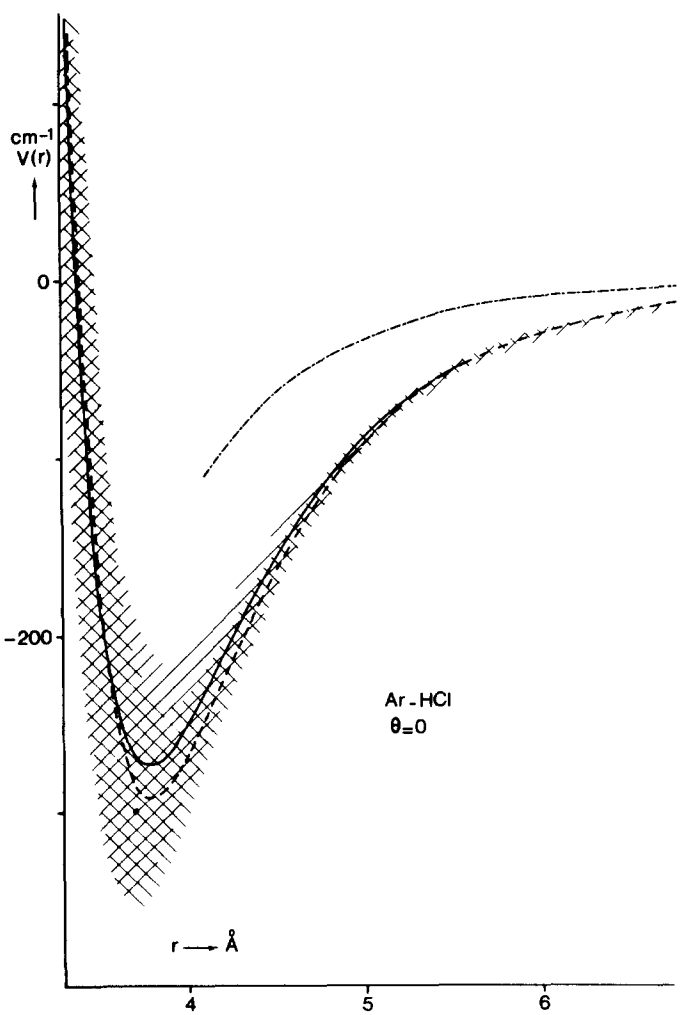

FIG. 3. HCl–Ar potential for $\theta=0°$. Best fits as calculated in this article A1— — — with error ; A2 —— with error compared with a Multipole expansion — - —.

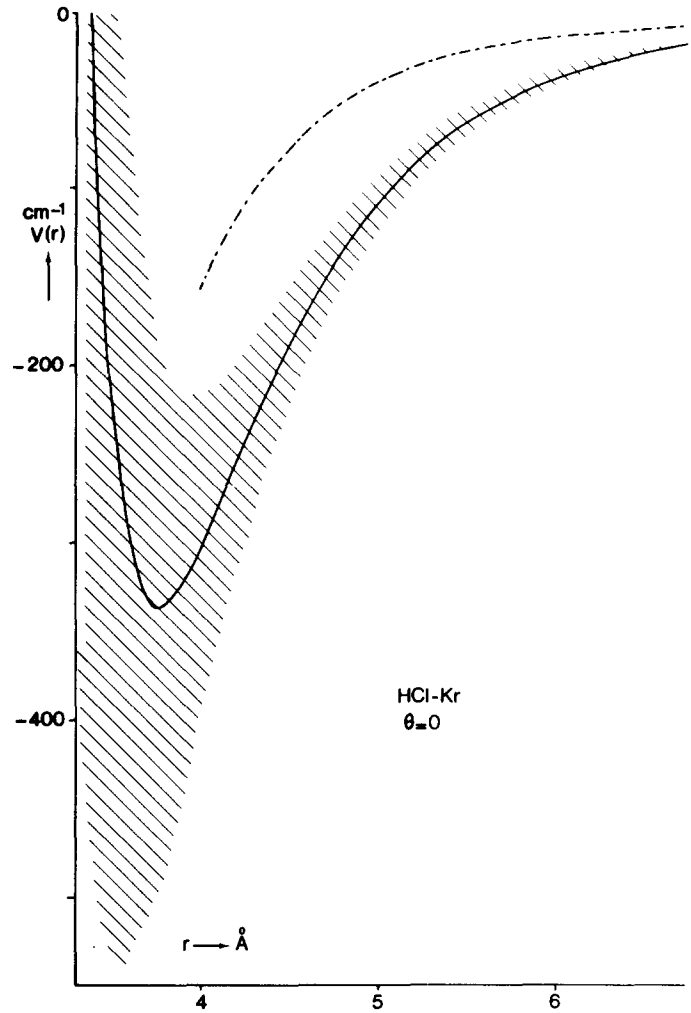

FIG. 4. HCl–Kr potential for $\theta=0°$. Best fit potential K —— with error compared with multipole expansion — — — — —.

scription of the short-range behavior of the anisotropic potential. We are now in a position to test this assertion directly.

Buckingham[16] has given the following expression for the leading terms in a multipole expansion of the anisotropic interaction between a linear and a spherical molecule:

$$V(r,\theta) = -(2C_{6i}+C_{6D})r^{-6} - P_1(\cos\theta) \times[36/5\,C_{6i}(\theta_1/\mu_1)+6/5\,C_{6D}(A_{\parallel}+2A_{\perp}/\alpha)_1]r^{-7} - P_2(\cos\theta)[2\,C_{6i}+C_{6D}(\alpha_{\parallel}-\alpha_{\perp}/3\alpha)_1]r^{-6}+\cdots\,, \tag{16}$$

with $C_{6i}=1/2\,\alpha_2\mu_1^2$ and $C_{6D}=3/2(U_1U_2/U_1+U_2)\alpha_1\alpha_2$. The values of the constants for molecule 1 (HCl) and molecule 2 (Ar, Kr) are given in Table V. In Figs. 5 and 6 the $l=1$ and $l=2$ parts of the multipole series are compared with the corresponding parts of the best fit potentials. As can be seen the multipole series differs significantly from the best fit potentials, even at larger distances, where the attractive parts of the potentials A1, A2, and K are dominant. Apparently, a pressure broadening experiment probes the HCl–noble gas inter-

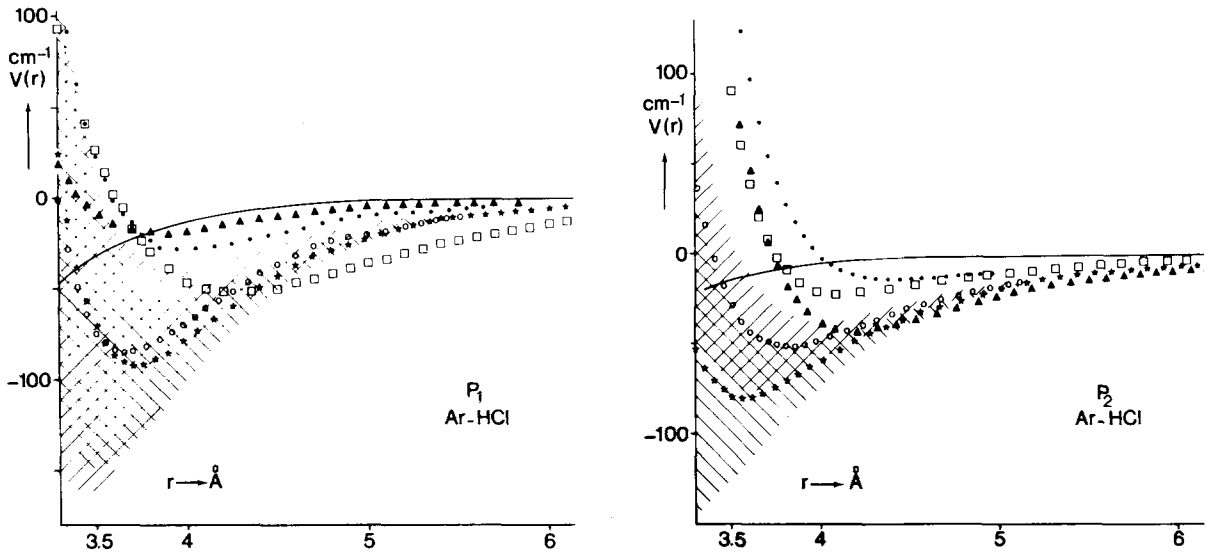

FIG. 5. P_1 and P_2 parts of the calculated HCl–Ar potentials. Best fits as calculated in this work A1* with error \\\ and A2 o with error /// compared with ●e, □ HWK1, ▲ HWK2, and —— multipole (see text).

molecular potential in a region over which the first few multipole terms are not sufficient to give an adequate description of the intermolecular potential.

It is instructive to compare the best fit Ar–HCl and Kr–HCl potentials, A2 and K, respectively. (We prefer to compare K with A2, because the isotropic parts of these two potentials were generated according to the same prescription.) From Table I one can see that the anisotropic potential parameters for the two systems are of the same order or magnitude, the Kr–HCl parameters being, however, smaller in all cases. Taking the error estimates into account, one notes that the difference between the P_1A or P_1R parameters for both systems is not significant. The difference between the sets of P_2A and P_2R parameters (in particular the latter) is somewhat larger and one is therefore tempted to conclude that the anisotropic parts of the HCl–noble gas potentials do not seem to scale as the isotropic potentials. If the multipole expansion [Eq. (16)] described the attractive part of the potential adequately, one would expect the values for P_1A and P_2A shown in Table I. Clearly, the "experimental" P_1A and P_2A coefficients differ both in magnitude and in their trend with the noble gas partners, from the multipole prediction. This is an extra indication that the first few terms of the multipole series have little relevance for the attractive part of the HCl–noble gas potential in the region under consideration.

Over the last few years, anisotropic potential surfaces for the Ar–HCl system have been proposed by a number of authors, on the basis of different pieces of experimental information. Neilsen and Gordon[4] compared the results of semiclassical trajectory calculations with the following experimental data: the pressure broadening of the 5 lowest HCl rotational dipole transitions at room temperature,[17] the pressure induced shift

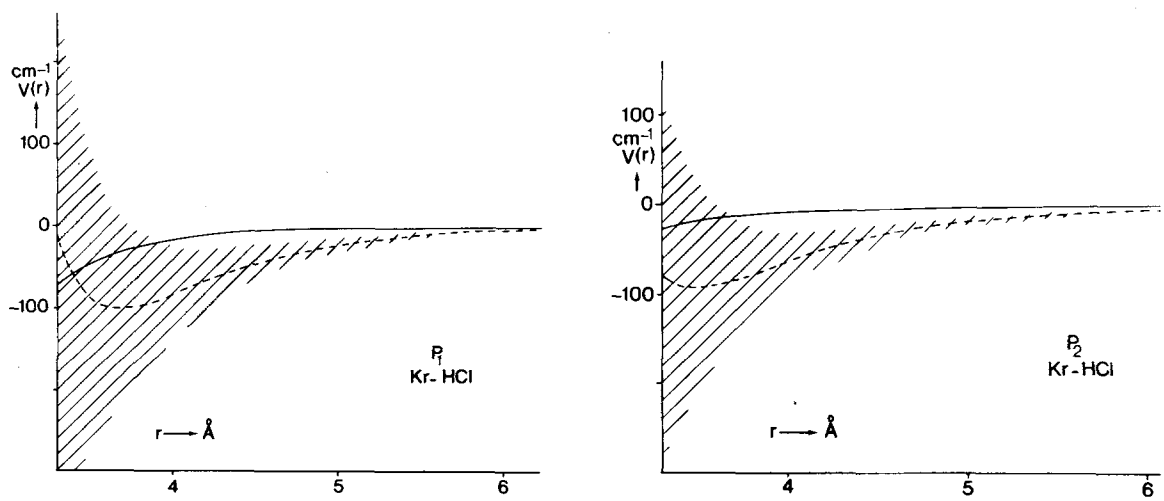

FIG. 6. P_1 and P_2 parts of the best fit potential for HCl–Kr as calculated in this work, - - - K with error /// compared with a multipole expansion ——.

TABLE IV. Values of the well depth and the distance at that point with $\theta = 0°$ for the full potentials and the P_1 and P_2 parts, with the calculated upper and lower bounds. Note that these calculated extremes can exit the physical region.

	A1			A2			K		
r(Å)	3.70	3.80	3.90	3.65	3.75	3.90	3.55	3.75	3.95
ϵ(cm^{-1})	357.2	291.3	238.7	349.5	273.5	215.0	538.0	336.1	217.0
r_1	3.50	3.75	3.90	3.40	3.65	3.95	3.15	3.65	4.15
ϵ_1	147.7	91.1	56.3	163.2	84.6	40.8	357.0	99.9	27.6
r_2	3.25	3.60	3.80	3.60	3.80	4.0	2.10	3.50	4.05
ϵ_2	143.0	79.3	51.6	76.3	51.4	37.4	2000.	93.0	30.3

of the $j = 0 \rightarrow 1$ rotational dipole transition at room temperature[18] and the pressure dependence of the longitudinal relaxation time of the HCl–proton between 304°K and 423°K.[19] The isotropic Ar–HCl potential that was used in Ref. 4 was a modified Buckingham version of Eq. (14). Although Neilsen and Gordon observe that a full numerical optimization of the anisotropic potential parameters would be prohibitively expensive, they did study the variation of the computed cross sections with the anisotropic potential parameters for a number of points in parameter space. Using the information thus obtained Neilsen and Gordon were able to estimate the anisotropic potential parameters that would yield an optimum fit with the experimental data mentioned above. The parameters characterizing this potential (potential "e" of Ref. 4) are given in Table I. Using this Neilsen and Gordon fully optimized potential in the SGC model, we generated cross sections for line broadening that agree very well with the more recent experimental low temperature data, though, surprisingly enough, somewhat worse with the older room temperature data (Fig. 1, Table II). Comparing the $l = 1, 2$ parts of potential e with the corresponding parts of our best fit potential A1 (Fig. 5) one observes a large difference. Potential e is invariably shallower than A1, and has moreover its minimum a larger r. Although some discrepancy was to be expected because e and A1 have different isotropic parts, the difference between A1 and e is certainly much larger than the difference between A1 and A2 (the latter of which has an isotropic part rather similar to e). Molecular beam electric resonance spectroscopy on Ar–HCl van der Waals molecules[20] has yielded new and accurate experimental data that provide a sensitive test for the Ar–HCl anisotropic potential. Using a close-coupling method, Dunker and Gordon[21] have computed a number of ground state and excited state properties of the Ar–HCl complex, using the Neilsen–Gordon fully optimized potential e. The properties of the dimer, predicted with this potential surface, turn out to be in striking disagreement, with the experimental results of Ref. 20. Recently, Holmgren and Klemperer[9] have developed a very efficient approximate method to compute the ground state properties of the van der Waals dimers. Using this method, they have analyzed the available electric resonance data on the dimers of Ar with $H^{35}Cl$, $H^{37}Cl$, $D^{35}Cl$, and $D^{37}Cl$. From a numerical nonlinear least squares minimization, these authors obtained two distinct anisotropic potential surfaces that both reproduce the electric resonance data to within experimental accuracy. The parameters characterizing these two potential surfaces (hereafter referred to as HWK1 and HWK2) are given in Table I. Using the SGC model, we generated the Ar–HCl rotational line broadening cross sections for the HWK1 and HWK2 potentials. As can be seen from Fig. 1 (Table II) the agreement with the experimental cross sections is equally poor for both potentials. The $l = 1$ and $l = 2$ parts of the HWK1 and HWK2 potentials are compared with the corresponding

TABLE V. Molecular constants.

	$\alpha(10^{-25}$ cm$^3)$	$(\alpha_{\parallel} - \alpha_{\perp})/3\alpha$	$\mu(10^{-18}$ esu·cm)	$\theta(10^{-26}$ esu·cm$^2)$	$A_{\parallel}/\alpha$ (10^{-8} cm)	$A_{\perp}/\alpha(10^{-8}$ cm)	U(eV)
HCl	26.3[a]	0.037[b]	1.1806[c]	3.74[d]	0.364[e]	0.057[e]	12.84[f]
Ar	16.4[g]						15.76[h]
Kr	24.8[g]						14.0[h]
HCl–Ar		$C_{6i} = 1.008(10^{-20}$ esu^2 Å$^5)$		$C_{6d} = 73.24(10^{-20}$ esu^2 Å$^5)$			
HCl–Kr		$C_{6i} = 1.524$ (10^{-20} esu^2 Å$^5)$		$C_{66} = 104.48(10^{-20}$ esu^2 Å$^5)$			

[a]Reference 11.
[b]Bridge and Buckingham, Proc. R. Soc. A **295**, 334 (1966).
[c]E. W. Kaiser; J. Chem. Phys. **53**, 1686 (1970).
[d]F. de Leeuw and A. Dymanus; J. Mol. Spectrosc. **48**, 427 (1973).
[e]D. Robert, C. Giradet, and L. Galatry; Chem. Phys. Lett. **3**, 102 (1969).
[f]Landolt-Börnstein, Zahlenwerte und Funktionen **3**, 360 (1951); **1**, 211 (1950).
[g]H. B. Levine and G. Birnbaum, J. Chem. Phys. **55**, 2914 (1971).

parts of potential A1 in Fig. 5. One observes that the HWK1 and HWK2 surfaces differ considerably from potential A1. In this case a direct comparison of the anisotropic parts is permittable because the isotropic part of our potential A1 is equal to the isotropic part of the HWK2 potential. It should be noted that the ground state properties of van der Waals molecules depend almost exclusively on the shape of the anisotropic potential surface around its absolute minimum. Rotational line broadening, on the other hand, is also sensitive to the short range repulsive, and the long range attractive parts of the potential. It is therefore not surprising that the potentials HWK1 and HWK2 fail to predict the line broadening correctly. It is, however, disconcerting to find that the potentials A1 and A2 differ so much from both the HWK1 and HWK2 potentials in the region of the potential minimum. In particular, it is almost certain that both A1 and A2, with absolute minima around 3.8 Å, will fail to predict the correct ground state equilibrium distance of Ar and HCl in the dimer (close to 4.0 Å).

V. CONCLUSIONS

The main conclusion that must be drawn from the results of the previous section is that in spite of the large amount of available experimental information on the Ar–HCl system, none of the anisotropic potential surfaces discussed above can make a strong claim to be close to the "true" Ar–HCl anisotropic potential surface The Neilsen–Gordon fully optimized potential *e* while in fair agreement with line broadening data, does not predict the dimer properties correctly. The Holmgren–Waldman and Klemperer potentials HWK1 and HWK2 which do describe the ground state properties of the dimer correctly, are found to predict unrealistic line broadening cross sections. The new optimized potential A1, obtained in the present work yields the correct line broadening cross sections, but is bound to predict the wrong equilibrium distance of the van der Waals molecule. Finally, the multipole series, which should describe the long range behavior of the intermolecular potential, disagrees with all of the above anisotropic potentials in the region of interest. The Kr–HCl potential surface determined in the present work (potential K) disagrees equally badly with the corresponding multipole expression, but no other "experimental" potentials are, at present, available for comparison. For this reason, we will restrict the remainder of the discussion to the Ar–HCl system.

At this stage, there are obviously two questions that we should attempt to answer. First of all, what are the possible causes for the large discrepancies between the different experimental potential surfaces? And secondly, in what way may one hope to pin down the Ar–HCl anisotropic interaction more accurately? One possible cause for the difference between potential A1 and the other experimental potentials might be the approximate nature of the SGC model. Smith, Giraud, and Cooper[7] have tested the model by comparing the results it yields for one particular potential surface, i.e., the Neilsen–Gordon potential "52",[23] with the results that Neilsen and Gordon obtain for this potential in full semiclassical trajectory calculation. For all but the lowest two rotational transitions, the agreement is found to be good. It is of course dangerous to extrapolate this agreement to any other anisotropic potential. However, the fact that we obtain fairly good agreement with the experimental linewidth when using the (very different) Neilsen–Gordon fully optimized potential *e* seems to indicate that the SGC model agrees with the Neilsen and Gordon results over a wide range in parameter space. A more likely cause for the discrepancy between the different potentials, is the neglect of higher order Legendre polynomial terms in the intermolecular potential. Although only $l=1$ and $l=2$ terms suffice to fit line broadening data or dimer properties separately, it may well be that more terms are needed to described all pieces of experimental information simultaneously. Theoretical calculations on the Ar–HCl anisotropic potential surface[24] seem to point in this direction.

It is clear that much could be learned from an attempt to fit the presently available line broadening (and related) cross sections and the dimer data simultaneously. However, more experimental information on the Ar–HCl system is available that deserves being taken into account. There is for instance the discrepancy between the well depth of the isotropic Ar–HCl potential, as determined by Farrar and Lee[8] and Holmgren *et al.*[9] ($E_{\min} = -132$ cm^{-1}) and the enthalpy of formation of Ar–HCl dimers as estimated from the temperature dependence of the infrared absorption of these dimers. ($\Delta H = 1.1 \rightarrow 1.5$ kcal/mole $= 385 \rightarrow 524$ cm^{-1}).[25–27] In this context it is interesting to note that the depth of the absolute minimum of potential A1 obtained in the present work is closed to 290 cm^{-1} with a lower bound close to 360 cm^{-1}. Boom *et al.*[27] have observed absorption peaks in the low temperature, low density, far infrared spectrum of Ar–HCl mixtures, which these authors ascribe to transitions between different excited states of the Ar–HCl dimer. Whereas the molecular beam electric resonance data of Refs. 8 and 9 provide information on the shape of the potential surface close to its minimum, the far infrared spectra of Ref. 27 should contain information about a larger part of the potential well. Thus far, the infrared spectra of the dimers have not been interpreted quantatively. However, using a simple anharmonic oscillator model, one has recently been able[28] to explain the main features of the far infrared spectra of the dimers. The results obtained, turn out to be consistent with the strong angle dependence of potential A1, but not with the much shallower potentials HWK1, HWK2 and *e*. Direct computation of the far infrared spectrum of Ar–HCl dimers at finite temperatures from knowledge of the anisotropic potential surface is feasible in principle. The actual calculations may however be quite time consuming because of the large number of states that are populated at the temperatures of the infrared experiments. This problem would be greatly reduced if selective spectroscopy on the internal degrees of freedom of Ar–HCl dimers could be performed (e.g., through excitation of dimers in a molecular beam with a tunable infrared laser). As yet, no such experiments have been performed.

ACKNOWLEDGMENT

The authors are very grateful to S. Holmgren, M. Waldman, and W. Klemperer for sending them preprints of their work. We wish to thank D. Gosman for letting us use the CDC 6400 computer of the Zeeman laboratorium in Amsterdam and M. Ryssenbeek for the helpful discussions on the use of minimization program package. This work is part of the research program of the Foundation for Fundamental Research of Matter (FOM) and was made possible by financial support from the Netherlands organization for Pure Research (ZWO).

[1]D. Robert, M. Giraud, and L. Galatry, J. Chem. Phys. **51**, 2192 (1969); M. Giraud, D. Robert, and L. Galatry, J. Chem. Phys. **57**, 144 (1972); **59**, 2204 (1973); P. Isnard, C. Boulet, D. Robert, and L. Galatry, Mol. Phys. **33**, 259 (1977).

[2]C. J. Tsao and B. Curnutte, J. Quant. Spectrosc. Radiat. Transfer **2**, 41 (1962).

[3]L. Jansen, Phys. Rev. **110**, 661 (1958).

[4]W. Neilsen and R. Gordon, J. Chem. Phys. **58**, 4131, 4149 (1973); W. Neilsen, thesis, Harvard, 1972.

[5]R. M. van Aalst, R. Spiekerman, and J. van der Elsken, Phys. Lett. A **47**, 451 (1974); R. M. van Aalst, J. Schuurman, and J. van der Elsken, Chem. Phys. Lett. **35**, 558 (1975).

[6]D. Frenkel, D. J. Gravesteyn, and J. van der Elsken, Chem. Phys. Lett. **40**, 9 (1976); D. Frenkel, thesis, Amsterdam, 1977.

[7]E. Smith, M. Giraud, and J. Cooper, J. Chem. Phys. **65**, 1256 (1976); *ibid.*, J. Chem. Phys. **66**, 376 (1977); E. Smith and M. Giraud, J. Chem. Phys. **66**, 1762 (1977).

[8]J. M. Farrar and Y. T. Lee, Chem. Phys. Lett. **26**, 428 (1974).

[9]S. L. Holmgren, M. Waldman, and W. Klemperer, J. Chem. Phys. **67**, 4414 (1977); Part II (preprint); William Klemperer, Faraday Discuss. Chem. Soc. **62**, 179 and 307 (1977).

[10]A. H. Stroud, *Numerical quadrature and solution of ordinary differential equations* (Springer, Berlin, 1974).

[11]J. O. Hirchfelder, C. F. Curtiss, and R. B. Bird, *Molecular Theory of gases and liquids* (Wiley, New York, 1954).

[12]J. Weeks, D. Chandler, and H. Andersen, J. Chem. Phys. **54**, 5237 (1971).

[13]R. J. Le Roy, J. Scott, and J. E. Grabenstetter, Faraday Discuss. Chem. Soc. **62**, 169 (1977).

[14]F. James and M. Roos, Comput. Phys. Commun. **10**, 343 (1975).

[15]P. R. Bevington, *Data reductional and error analysis* (McGraw Hill, New York, 1969), pp. 242.

[16]A. D. Buckingham, Adv. Chem. Phys. **12**, 107 (1967).

[17]H. A. Gebbie and M. W. B. Stone, Proc. Phys. Soc. London **82**, 309 (1963); H. Scott, thesis, Ohio, 1973.

[18]D. H. Rank, D. P. Eastman, B. S. Rao, and T. A. Wiggins, J. Mol. Spectrosc. **10**, 34 (1963); A. Ben-Reuven, S. Kimel, M. A. Hirschfeld, and J. H. Jaffe, J. Chem. Phys. **35**, 955 (1961).

[19]A. M. Leonardi-Cattolica, K. O. Prins, and J. S. Waugh, J. Chem. Phys. **54**, 769 (1971).

[20]S. E. Novick, P. B. Davies, S. J. Harris, and W. Klemperer, J. Chem. Phys. **59**, 2273 (1973); S. E. Novick, K. C. Janda, S. L. Holmgren, M. Waldman, and W. Klemperer, J. Chem. Phys. **65**, 1114 (1976).

[21]A. M. Dunker and R. G. Gordon, J. Chem. Phys. **64**, 354 (1976).

[22]D. Frenkel and J. van der Elsken, J. Chem. Phys. **67**, 4243 (1977).

[23]Actually, Smith, Giraud, and Cooper fitted a Lennard-Jones type anisotropic potential (like our potential A2) to the Neilsen–Gordon potential "52". The results of such a procedure depend, however, rather strongly on the weight function used in the least squares fit and, in general, fitting one potential surface to another should be avoided, if possible.

[24]The work of W. Stevens and D. Robert cited in Ref. 7.

[25]D. H. Rank, B. S. Rao, and T. A. Wiggens, J. Chem. Phys. **37**, 2511 (1962).

[26]A. W. Miziolek and G. C. Pimentel, J. Chem. Phys. **65**, 4462 (1976).

[27]E. W. Boom, D. Frenkel, and J. van der Elsken, J. Chem. Phys. **46**, 1826 (1977).

[28]E. W. Boom and J. van der Elsken, J. Mol. Struct. **45**, 113 (1978).